# A quantitative framework for interpretation of basal ice facies formed by ice accretion over subglacial sediment

Poul Christoffersen,[1,2] Slawek Tulaczyk,[1] Frank D. Carsey,[3] and Alberto E. Behar[3]

Received 30 June 2005; revised 2 November 2005; accepted 28 November 2005; published 4 March 2006.

[1] We have constructed a numerical model of basal ice formation for glacier ice in contact with subglacial sediment. The model predicts four different ice facies whose formation is controlled by availability of subglacial water to satisfy the basal freeze-on rate. Clean (or clotted) facies may result from congelation (or frazil) ice growth occurring when (supercooled) meltwater separates ice base from substrate or if a groundwater source can supply water to the ice base at a velocity equal to the freezing rate. Laminated facies develops when the supply of subglacial water is sufficiently constrained for cryostatic suction to raise the subglacial effective stress above a threshold for intrusion of ice into sediment by regelation. Debris laminas ($\sim$1 mm) are entrained by short, periodic regelation events (of a few hours) separated by longer periods (days to months) of congelation. Further meltwater limitation produces a massive dirty ice facies due to stacking of debris laminas. The model predicts growth of solid dirty ice facies when the bed is meltwater-depleted with fast freezing (5 mm $yr^{-1}$) causing enhanced erosion (30 mm $yr^{-1}$). We find that basal ice facies and sediment entrainment are controlled mainly by the ratio of freezing rate to water supply rate. The predicted ice facies compare favorably with borehole camera imagery of the basal ice layer in Kamb Ice Stream, West Antarctica. Facies variability in this layer suggests complex hydrologic history for the West Antarctic Ice Sheet with significant changes occurring over a period of several thousand years.

**Citation:** Christoffersen, P., S. Tulaczyk, F. D. Carsey, and A. E. Behar (2006), A quantitative framework for interpretation of basal ice facies formed by ice accretion over subglacial sediment, *J. Geophys. Res.*, *111*, F01017, doi:10.1029/2005JF000363.

## 1. Introduction

[2] Glaciers and ice sheets often contain a basal ice layer formed partly or wholly by subglacial accretion. The Byrd ice core in West Antarctica contained 4.8 m of frozen-on basal ice [*Gow et al.*, 1979]. This layer was composed mainly of stratified basal ice (Figure 1). The Camp Century ice core from Greenland had 15.7 m of stratified basal ice [*Herron and Langway*, 1979]. Basal ice layers are of considerable geologic importance because they provide observational constraints on the rate of glacial erosion and sediment transport [*Alley et al.*, 1997]. They may also be an important source of material for sedimentation, as illustrated, for instance, by the presence of ice rafted debris on the floor of the North Atlantic basin [*Heinrich*, 1988; *Bond et al.*, 1992]. Past interpretation of basal ice layers focused on the plausible hypothesis that the variability in their physical and chemical characteristics reflects spatial and temporal changes in subglacial thermal and hydrological conditions [*Weertman*, 1961; *Lawson and Kulla*, 1978; *Boulton and Spring*, 1986; *Souchez et al.*, 1987; *Sugden et al.*, 1987; *Jouzel et al.*, 1999; *Christoffersen and Tulaczyk*, 2003a, 2003b; *Souchez et al.*, 2003, 2004]. A quantitative framework for interpretation of basal ice facies is needed to interpret properties of basal ice layers in terms of long-term records of subglacial hydrological conditions, which are otherwise unconstrained. Recently, a borehole camera system developed at JPL was used to image basal ice in Kamb Ice stream, West Antarctica [*Carsey et al.*, 2002]. The imagery revealed an 8- to 14-m-thick debris-bearing basal layer. This observation was unexpected because it represents a several thousand year long history of basal ice accretion while melting was thought to dominate the basal thermal regime of fast flowing glaciers and in particular ice streams [*Alley et al.*, 1997; *Anandakrishnan et al.*, 2001]. The basal freezing rate of Kamb Ice Stream, enhanced by loss of frictional heat from cessation of fast ice flow ca. 150 years ago, is today about 4 mm $yr^{-1}$ [*Kamb*, 2001]. Hence only the lower 0.9 m of the basal ice layer was accreted poststagnation [*Vogel et al.*, 2005].

[3] In published models, stratified basal ice develops from (1) glaciohydraulic supercooling near steep glacial overdeepenings [*Alley et al.*, 1998; *Lawson et al.*, 1998; *Roberts et al.*, 2002], (2) multiple freezing events when ice slides over rigid bedrock [*Hubbard and Sharp*, 1993, 1995],

[1]Department of Earth Sciences, University of California, Santa Cruz, California, USA.
[2]Now at Centre for Glaciology, Institute of Geography and Earth Sciences, University of Wales, Aberystwyth, UK.
[3]Jet Propulsion Laboratory, California Institute of Technology, Pasadena, California, USA.

Copyright 2006 by the American Geophysical Union.
0148-0227/06/2005JF000363

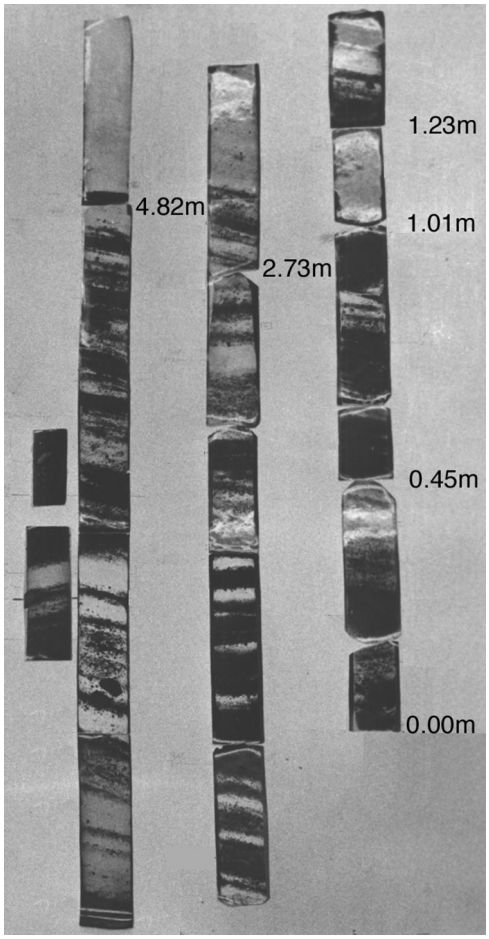


**Figure 1.** Photograph of basal ice in the Byrd ice core. Numbers refer to height (m) above core bottom (courtesy of A. J. Gow).

(3) regelation into the basal sediment [*Iverson*, 1993; *Iverson and Semmens*, 1995; *Iverson*, 2000], and (4) deformation near ice margins [*Knight*, 1994, 1997; *Waller et al.*, 2000]. Here, we use a numerical ice-till continuum model to show that different types of stratified basal ice may also develop from subglacial frost-heave processes. We compare model output to the JPL borehole camera imagery. This approach benefits from the fact that basal properties of West Antarctic ice streams are relatively well known [*Anandakrishnan and Alley*, 1997; *Anandakrishnan et al.*, 2001; *Bindschadler et al.*, 2001; *Kamb*, 2001; *Raymond et al.*, 2001; *Bindschadler et al.*, 2003]. Numerous borehole experiments have been conducted between 1988 and 2000 [*Engelhardt and Kamb*, 1997, 1998; *Kamb*, 2001], subglacial sediment has been sampled and analyzed [*Kamb*, 1991; *Tulaczyk et al.*, 1998, 2000, 2001] and it is evident that low basal shear stresses give rise to virtually no internal deformation within ice streams [*Engelhardt and Kamb*, 1998]. Isotopic analysis of an ice core spanning the transition from glacial ice to basal ice in Kamb Ice Stream shows that the basal ice layer is composed of refrozen glacial meltwater [*Vogel et al.*, 2005]. Our quantitative accretion model has been set up to include processes that are selected to represent primary conditions at the basal interface of a freezing ice mass and within a subglacial layer of till. Despite the variable nature of subglacial environments (e.g., ice resting on bedrock or overlying widespread subglacial drainage systems or lakes), our model is not meant to cover all-encompassing simulations of every possible subglacial environment. However, we show that even this simplified model of a single subglacial environment, i.e., ice base freezing over a layer of till, can reproduce a range of basal ice facies, which are in general similar to those observed in nature. We find that the most important control on formation of different basal ice facies is the ratio of basal freezing rate to water supply rate.

## 2. Application of Frost Heave Theory in Glaciological Models

[4] Basal freeze-on beneath glaciers and ice sheets can be formalized by adaptation of frost heave treatment [*Christoffersen and Tulaczyk*, 2003a, 2003b]. *O'Neill and Miller* [1985] conjectured that growth of ice into the sediment pore spaces is inhibited by capillary pressure arising at curved ice-water interfaces. More recently, *Rempel et al.* [2004] proposed a new microphysical explanation for frost heave based on premelting dynamics and associated intermolecular forces. This new model represents a generalization of the previous, phenomenological treatment of frost heave, mainly due to specific inclusion of the influence of ice saturation in the frozen fringe on heaving rates and ice lens initiation. When the influence of ice saturation on interfacial force is null, the key equations proposed by *Rempel et al.* [2004, equation (3.4) and (3.10)] simplify to those of *O'Neill and Miller* [1985]. Even when this is not the case, the difference between the two models is relatively minor. Quantitative differences between these two models are examined more closely in Appendix A.

[5] The premelting model by *Rempel et al.* [2004] represents a significant advancement in understanding of frost heave microphysics. However, its reliance on knowledge of spatial distribution of ice saturation makes it difficult to apply at this point in time because of dearth of relevant observational constraints. Usage of ad hoc parameterizations does not appear to be better than application of the older frost heave model [*O'Neill and Miller*, 1985], which has been successfully used in both experimental and theoretical work conducted over several decades [*Miller*, 1973; *O'Neill*, 1983; *O'Neill and Miller*, 1985; *Fowler and Krantz*, 1994; *Krantz and Adams*, 1996; *Miyata*, 1998; *Miyata and Akagawa*, 1998]. In the Appendix we show that O'Neill and Miller's phenomenological frost heave model, although not fully correct in identifying microphysical causes of frost heave, can be used as an acceptable approximation by folding the greater complexity of the premelting model [*Rempel et al.*, 2004] into simpler terms. Whatever the exact physical reason for the interfacial pressure inhibiting ice growth into pore spaces, the inhibiting pressure term can simply be incorporated as a control parameter into the generalized Clapeyron equation (see equation (1)). Furthermore, if spatial distribution of ice saturation is dependent on pore and particle size distribution, as it is reasonable to expect, the capillary pressure analogy used by *O'Neill and Miller* [1985] may effectively, if not in terms of physical explanation, be close to the approach of *Rempel et al.* [2004].

[6] The novel approach of *Rempel et al.* [2004] represents a microphysically correct generalization of O'Neill and Miller's model but it does not undercut result based on that model (see Appendix A and *Clarke* [2005]). The freeze-on theory proposed by *Christoffersen and Tulaczyk* [2003a] is supported by isotopic data for basal ice in East Antarctic outlet glaciers [*Souchez et al.*, 2004] in addition to observations of 0.35°C supercooling beneath Kamb Ice Stream [*Kamb*, 2001, sections 3.1, 4.6 and 8.3]. We thus adhere to an empirical methodology whereby findings can be parameterized to suit large-scale purposes. The versatility of this approach is demonstrated by *Bougamont et al.* [2003a, 2003b]. They modified the basal freeze-on model by *Christoffersen and Tulaczyk* [2003a] and showed how a complex one-dimensional (1-D) model can be simplified to fit the theoretical framework of a 2-D flow line solution. This work yielded key new insights to ice stream behavior by showing that the stoppage of Kamb Ice Stream, ~150 years ago, may be a result of inherent flow periodicity controlled by basal freeze-on switching on and off. Analysis of basal ice sampled from Kamb Ice Stream supports this finding [*Vogel et al.*, 2005].

## 3. Theoretical Framework

### 3.1. Numerical Model

[7] We use a numerical 1-D model to investigate accretionary basal ice growth in situations where a freezing ice base rests on a water-saturated sediment similar to the till layer observed beneath Siple Coast ice streams [*Tulaczyk et al.*, 1998; *Kamb*, 2001]. Till cores sampled from beneath Whillans, Kamb and Bindschadler Ice Steams invariably consist of dark grey, wet, very sticky, clay-rich diamicton [*Kamb*, 2001] interpreted by *Tulaczyk et al.* [1998] as a glacial till. A new theoretical outline of basal freeze-on is given by *Christoffersen and Tulaczyk* [2003a] and its implication on ice flow in West Antarctica is discussed by *Bougamont et al.* [2003b]. Previously, we predicted that fast freezing associated with ice stream stoppage should result in a solid basal ice facies composed of decimeter-scale layers of frozen-on sediment separated by lenses of clean segregation ice. We used a generalized form of the Clapeyron equation and a control parameter, $\sigma_f$, representing interfacial pressure, to simulate coupled flow of water, heat and solutes in unfrozen sediment beneath a freezing ice base with temperature given by

$$T = -\frac{273.15}{L}\left(\frac{1}{\rho_i}-\frac{1}{\rho_w}\right)p_w - \frac{273.15}{L\rho_i}\sigma_f - \frac{273.15}{L\rho_w}p_o \quad (1)$$

where $L$ is coefficient for latent heat of fusion, $\rho_i$ and $\rho_w$ are the densities of ice and water, $p_w$ is water pressure, $\sigma_f$ is interfacial pressure inhibiting ice growth into pore spaces, and $p_o$ is osmotic pressure, which can be determined from the solute content in the pore water [*Christoffersen and Tulaczyk*, 2003a]. *Raymond and Harrison* [1975] used the same equation to investigate water in veins between ice crystals [see also *Hooke*, 1998, p. 5]. The freezing rate, $f$, at the ice base is calculated from the basal heat budget, which is

$$f = \frac{\theta_b K_i - G - \tau_b U_b}{\rho_i L} \quad (2)$$

where $\theta_b$ is the basal ice temperature gradient ($\partial T/\partial z$ with $z$ being vertical coordinate), $K_i$ is thermal ice conductivity coefficient, $G$ is geothermal heat flux, $\tau_b$ is basal shear strength and $U_b$ is basal ice velocity.

[8] A deficit in the basal heat budget arises from supercooling as observed at the base of Kamb Ice Stream where temperatures in two boreholes were measured at −0.35°C below the pressure-melting point (calculated as $T_{pmp}$ = −0.71°C for 1057-m-thick ice) [*Kamb*, 2001]. Ice-water phase equilibrium prescribed through equation (1) shows that supercooling induces hydraulic gradients. Subglacial pore water will thus flow toward the ice base where it accretes as a layer of basal ice. The basal ice layer grows continuously as long as the hydrological system can supply enough water to satisfy the basal heat budget (equation (2)). Darcy's law [e.g., *Domenico and Schwartz*, 1990, equation (4.53)] is used to prescribe vertical transport of water in the simulated system. Water pressure gradients arise when temperature is depressed below the pressure-melting point, $T_{pmp}$, which can be calculated by the first term of equation (1). The flows of heat and solutes are calculated by standard diffusion-advection equations [e.g., *Domenico and Schwartz*, 1990, equations (9.21) and (13.9)]. Theoretical details for coupled flows of water, heat and solutes beneath a freezing ice base are given by *Christoffersen and Tulaczyk* [2003a, 2003b].

### 3.2. Availability of Subglacial Meltwater

[9] Meltwater needed for the release of latent heat may be supplied to the ice base by a basal water system, pore water stored in the till layer, and/or deep subglacial groundwater. We make the assumption that an ice base experiencing long-term freezing on a widespread basis will be in contact with subglacial sediment and that deep subglacial groundwater and water stored in the pore spaces of a till layer are the main (i.e., continuously present) sources of latent heat. This generalization may constitute an end-member case, but it is plausible to assume that widespread basal freezing should inhibit development and maintenance of an organized subglacial drainage systems by promoting channel closure due to reduced water pressures and freezing on channel walls [*Clarke and Blake*, 1991; *Flowers and Clarke*, 2002; *Copland et al.*, 2003]. This should be particularly the case where basal freezing takes place beneath stopped ice streams, which still have relatively low horizontal water pressure gradients and thus small viscous heat dissipation that could counteract the effects of freezing and creep closure.

### 3.3. Entrainment of Debris by Regelation

[10] It is well known that regelation around hard bedrock bumps contributes to glacier sliding [*Weertman*, 1964] and sediment intake to temperate [e.g., *Hubbard and Sharp*, 1993] as well as polar ice masses [e.g., *Cuffey et al.*, 2000]. Regelation can also cause downward infiltration of ice into subglacial sediment as demonstrated experimentally by *Iverson* [1993] and *Iverson and Semmens* [1995], who showed that the infiltration rate can be determined by:

$$V_r = K_r \frac{p'}{d} \quad (3)$$

where $K_r$ is conductivity of sediment to ice, $p'$ is effective stress, and $d$ is the penetration depth of ice into the sediment. The rate of regelation decreases with increasing debris thickness because ice must regelate around all entrained particles [*Alley et al.*, 1997]. In earlier work, we may have underestimated the effect of regelation because we assumed (for computational simplicity) that water pressure throughout the till layer would adjust instantaneously to intrusion of ice by regelation. It appears that this approach represented an oversimplification. In our modified model, we treat explicitly the adjustment of vertical water pressure distribution in response to infiltration of ice by regelation as discussed in more detail below.

[11] Regelation of ice into subglacial sediment does not take place until the water pressure has dropped to a level where effective stress ($p' = p_i - p_w$ where $p_i$ is ice pressure and $p_w$ is water pressure) overcomes pressure associated with interfacial curvature and premelting effects. An effective regelation threshold ($\zeta > 0$) can be expressed formally through the specific surface area of till particles [*Tulaczyk*, 1999]. The existence of a regelation threshold may explain why regelation did not occur for $p' < 50$ kPa when Iverson and Semmens tested a silt-dominated till [*Alley et al.*, 1997]. The regelation threshold, $\zeta$, has for sub-ice stream till been estimated to be 100 kPa [*Tulaczyk*, 1999]. Measurements of specific surface area from adsorption data using the Brunauer, Emmett and Teller (BET) method [*Gregg and Sing*, 1982], conducted as a part of this study, indicate that $\zeta$ in some cases could exceed 1 MPa. Such high value may, however, not represent till behavior wholly because ice may form preferentially in pore spaces around larger particles rather filling micron-sized pore spaces. Until we know more about preferential freezing, we thus adhere to the earlier estimate ($\zeta = 100$ kPa) and make the assumption that $\sigma_f = \zeta$ [*Tulaczyk*, 1999].

[12] Regelation thresholds may require development of high effective stress before sediment is entrained. Widespread regelation into subglacial sediment is thus unlikely beneath fast moving ice streams where effective stresses are just 1–10 kPa [*Kamb*, 2001; *Tulaczyk et al.*, 2001]. Basal freeze-on may become a driver of regelation due to progressive increase in effective stress following extraction and consumption of subglacial water [*Christoffersen and Tulaczyk*, 2003a]. From past work, little is known about freeze-on driven regelation, but it is a potentially powerful mechanism because ice accretion will prompt dispersal of entrained particles and thereby enhance the rate of regelation as solid particles no longer have to push previously entrained debris ahead of them. Although basal freeze-on can enhance regelation, the two processes act also as competing mechanisms. The reason behind this contrast is that freeze-on causes consolidation of underlying sediments while regelation triggers swelling. In our modified model we use compressibility equations derived from laboratory experiments on till cores to simulate the pore water pressure variations in subglacial sediment undergoing freezing and regelation simultaneously.

### 3.4. Till Compressibility

[13] When regelation ice intrudes the pore spaces of basal sediment, the underlying material swells because less pore space is available for the amount of water in the system [*Clarke*, 1987; *Tulaczyk et al.*, 2000; *Kamb*, 2001; *Clarke*, 2005]. In our modified model, swelling occurs as a perturbation of the water pressure at the freezing interface. The increase in water pressure depends on the volume of pore space taken up by regelation ice and the penetration depth of the water pressure pulse is controlled by its size and by hydraulic properties of the subglacial sediment. Our improved model also features the use of compressibility equations to determine the volumetric behavior of the subglacial sediment allowing us to realistically simulate a wider range of basal ice facies. The equations are derived from triaxial experiments and consolidation tests using till cores sampled from beneath Whillans Ice Stream [*Tulaczyk et al.*, 2000]. They are

$$e_{NCL} = 0.78 - 0.125 \log(p'/p_0) \tag{4a}$$

$$e_{URL} = 0.57 - 0.02 \log(p'/p_0) \tag{4b}$$

where $e$ is void ratio (given by $e = \phi/(1-\phi)$ with $\phi$ being porosity), $p'$ is effective stress and $p_0 = 1000$ Pa. NCL refers to the normal consolidation line, which represents volumetric behavior of consolidating till with no preloading history. URL refers to the unloading-reloading line, which characterizes the volumetric behavior for the same material in an overconsolidated state. The latter equation is modified from *Tulaczyk et al.* [2000] and represents unloading at $p' = 100$ kPa, which corresponds to our assumed regelation criterion ($\zeta = 100$ kPa).

### 3.5. Formation of Clean, Dirty and Stratified Basal Ice Facies

[14] Changes in till porosity from consolidation induced by congelation ($T < T_{pmp}$; $p' < \zeta$) and swelling caused by regelation ($T < T_{pmp}$; $p' \geq \zeta$) can be calculated from equations (4a) and (4b). Figure 2a shows schematic diagrams of four types of stratified basal ice (I–IV). Figure 2b illustrates how till compressibility should govern formation of these ice facies. When freezing is first induced, clean ice (Figure 2a, type I) will accrete onto the ice base while the till progresses down the normal consolidation line, NCL (Figure 2b, type I). When the regelation criterion ($\zeta$) is reached, dirty regelation ice forms in the till pores near the ice base. The underlying till swells in response by moving up the unloading-reloading line, URL (Figure 2b, type II). Excess water pressure diffuses downward from the freezing interface and regelation terminates because the effective stress drops below the regelation criterion leaving a debris lamina in the overlying ice. Continued freezing will drive the effective stress back toward the regelation threshold by moving down the URL while clean ice accretes onto the entrained debris lamina. If this process becomes periodic a laminated ice facies is produced (Figure 2a, type II). The same cyclic process may, however, also develop a massive facies if all clean congelation ice ends up regelating into underlying sediment after its formation (Figure 2a, type III). Debris should still entrained periodically, but the stratigraphy is lost because debris-rich laminas stack up. The water pressure should then fluctuate within a narrow range close to the regelation threshold (Figure 2b, type III). This may cause insufficient supply of water to the ice base,

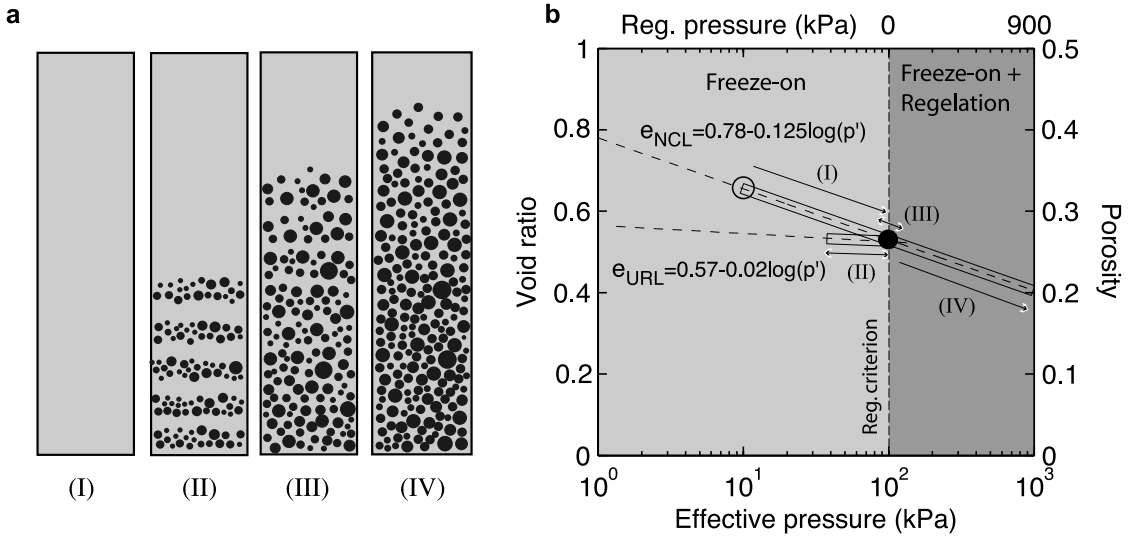


**Figure 2.** Schematic diagrams of basal ice illustrating (a) clear facies (type I), laminated facies (type II), massive facies (type III), and solid facies (type IV). Compressibility of sub-ice steam tills (Figure 2b) with NCL and URL referring to normal and overconsolidated conditions (modified after [*Tulaczyk et al.*, 2000]. Roman numerals (I–IV) correspond to basal ice facies I–IV outlined in Figure 2a.

particularly if freezing rates are high. Freezing may thus become a run-away process with pore water pressure dropping continuously as the till migrates down the NCL (Figure 2b, type IV) while a solid dirty ice facies forms from permanent regelation (Figure 2a, type IV).

## 4. Model Results

[15] We use a 1-D finite difference model to simulate a freezing ice-till continuum. Key model parameters and constants relevant for this study are listed in Table 1. Initial conditions are a low effective stress ($p' = 4$ kPa) that yields low basal shear strength ($\tau_b = 2$ kPa) and a high porosity ($\phi = 40\%$). In contrast to earlier work, we do not investigate effects from frictional heat related to ice motion. Water is driven out of the till via a freezing rate prescribed through a constant basal ice temperature gradient and a suite of experiments is set up to explore growth of basal ice under different types of subglacial conditions. Each experiment is characterized by a period of time during which the till layer consolidates progressively (equation (4a)) while a layer of clean basal ice develops as pore water freezes onto the ice base. The ultimate thickness of this layer depends on how fast the freezing rate can produce conditions suitable for regelation ($p' > \zeta = 100$ kPa). The triggering of debris entrainment by regelation provides a strong perturbation to the system (equation (4b)). It takes the model almost one year to reach a semisteady state from which consistent debris-bearing ice facies develop. The simulations cover a minimum of eight years of sediment entrainment. The time step is 6 minutes due to nonlinearities captured by the model, which has 100 nodes spaced at 0.01 m. Further

**Table 1.** Symbols and Values for Time-Dependent Model Parameters and Constants

| Symbol | Value | Definition |
|---|---|---|
| $c_v$ | $10^{-8}$ m$^2$ s$^{-1}$ | hydraulic diffusion coefficient |
| $f$ | [0, 6] $\times$ $10^{-3}$ m yr$^{-1}$ | freezing rate[a] |
| $G$ | 70 $\times$ $10^{-3}$ J s$^{-1}$ m$^{-2}$ | geothermal heat flux |
| $H$ | 1000 m | ice thickness |
| $K_h$ | $10^{-10}$ m s$^{-1}$ | hydraulic conductivity coefficient |
| $K_r$ | 2 $\times$ $10^{-15}$ m$^2$ Pa$^{-1}$ s$^{-1}$ | conductivity coefficient for regelation |
| $L$ | 3.34 $\times$ $10^5$ J kg$^{-1}$ | coefficient for latent heat of fusion |
| $p_i$ | 9.0 $\times$ $10^6$ Pa | ice pressure[b] |
| $p_w$ | 9.0 $\times$ $10^6$ Pa | water pressure[b] |
| $p'$ | 4.0 $\times$ $10^3$ Pa | effective stress[b] |
| $T_b$ | $-0.7$°C | temperature at ice base[b] |
| $\phi$ | 40% | porosity[b] |
| $\rho_i$ | 916 kg m$^{-3}$ | density of ice |
| $\rho_w$ | 1000 kg m$^{-3}$ | density of water |
| $\sigma_{iw}$ | 3.4 $\times$ $10^{-4}$ J m$^{-2}$ | Specific surface energy of ice-water interface |
| $\theta_b$ | [0.04, 0.06] °C m$^{-1}$ | Basal ice temperature gradient[a] |
| $\zeta$ | 100 $\times$ $10^3$ Pa | Regelation threshold criterion |

[a]Forcing parameter with numbers in brackets referring to end-member values.
[b]Model variable with number referring to initial value.

nodes are not needed in this study because water pressure fluctuations occur only in the upper half of the model domain. We have conducted 15 model runs to cover basal ice formation in a spectrum of subglacial conditions. The two boundary conditions that we vary are (1) basal ice temperature gradient and (2) influx of external water to the simulated system. The former prescribes the basal freezing rate; the latter determines water availability. Their nondimensional ratio can be treated as a single forcing parameter. The model predicts four different facies of stratified basal ice. These are designated: clear, laminated, massive, and solid basal ice. Steady state growth of clear ice constitutes in our model a trivial case where the influx of external water to the simulated system satisfies the heat budget causing no porosity changes in the till. Clear congelation ice may also form if the ice is separated from the bed due to influx of excess basal meltwater, although a clotted frazil ice facies may form if the latter becomes supercooled [*Lawson et al.*, 1998]. Below, we discuss in detail results of three model runs, which represent formation of debris-bearing basal ice facies formed by ice accretion. The three cases represent situations where the basal ice temperature gradient, $\theta_b$, is 20%, 50% and 80% steeper than the gradient resulting in neither melting nor freezing (0.033°C m$^{-1}$). The middle case corresponds to the present state of Kamb Ice Stream ($\theta_b$ = 0.052°C m$^{-1}$) [*Kamb*, 2001]. The assumed geothermal heat flux is $G$ = 0.070 W m$^{-2}$ [*Engelhardt*, 2004].

[16] The first model run shows how laminated basal ice may develop from periodic regelation events (Figures 3a–3e). The influx of groundwater to the system is in this case 95% of the freeze-on rate of $f$ = 1.4 mm yr$^{-1}$. The ice temperature gradient is 0.04°C m$^{-1}$. It takes roughly 1200 years of freezing for the effective stress to grow from initial conditions ($p'$ = 4 kPa) to the regelation criterion ($\zeta$ = 100 kPa). In this period, ~1.7 m of clean congelation ice accretes onto the ice base. Figure 3a shows cyclic fluctuations in regelation pressure ($p_r = p' - \zeta$). The amplitude peaks at ~0.9 kPa during the regelation events, which last just 8–9 hours (Figures 3a and 3b). About 0.3 mm of dirty ice forms during each event (Figures 3c and 3d). These regelation events are separated by longer periods of congelation (80–90 days). The ratio between growth rate of regelation ice and growth rate of congelation ice is ~0.7. The fluctuating debris content of laminated basal ice is seen in Figure 3e where C refers to congelation ice and R refers to regelation ice.

[17] The second model run illustrates growth of massive regelation ice (Figures 3f–3j). The influx of subglacial water is in this case 50% of what is required to satisfy the freezing rate of 3.6 mm yr$^{-1}$ induced by a basal ice temperature gradient of 0.05°C m$^{-1}$. It takes about ~43 years for effective stress to reach the regelation threshold ($\zeta$ = 100 kPa), and in this period ~0.16 m of clean congelation accretes onto the ice base. Regelation is still cyclic. A few debris bands develop (Figure 3f) but debris bands begin to stack up early in the simulation because an increase in effective stress speeds up regelation. The regelation pressure peaks at ~0.06 kPa before stacking causes a significant slow down of the regelation rate (Figure 3g). The thickness of the regelation ice layer increases gradually (Figure 3h) in a step-like way (Figure 3i). In this simulation, regelation events last only ~2.5 hours. Each event produces just ~0.01 mm of regelation ice. However, the periods of clean congelation ice growth are also very brief (~5.4 hours). All congelation ice refreezes into regelation ice. The ratio between regelation ice growth and congelation ice growth is ~3. The end result is a massive regelation ice facies containing ~50% debris by volume (Figure 3j).

[18] The third model run (Figures 3k–3o) illustrates the growth of solid dirty regelation ice. We do not allow any external water into the ice-till system. All latent heat must be supplied by pore water in the till. A basal temperature gradient of 0.06°C m$^{-1}$ produces a freeze-on rate of 5.8 mm yr$^{-1}$. The effective stress increases rapidly under these conditions so it takes just ~9 years to reach the regelation criterion (100 kPa). In this period ~0.052 m of clean congelation ice accretes onto the ice base. The regelation pressure continues to increase ($p' > \zeta$ = 100 kPa) because freeze-on has become a run away process (Figure 3k) with small fluctuation in effective stress of ~0.035 kPa (Figure 3l). The regelation ice layer thickens fast (Figure 3m) and linearly (Figure 3n). The ratio of the regelation rate to the freezing rate is ~6. The result is a solid dirty ice facies (frozen till) with a sediment content >60% by volume (Figure 3o).

## 5. Borehole Camera Imagery

[19] Figures 4a–4d show images of basal ice from Kamb Ice Stream obtained with the JPL borehole probe in the austral summer 2000–2001 [*Carsey et al.*, 2002]. The basal ice layer was observed in three boreholes and measured ~8–14 m in thickness. Isotopic analysis on an ice core segment shows that the basal ice is composed of refrozen glacial meltwater and that the transition from bubbly, meteoric glacier ice to accreted, debris-laden basal ice occurs within a few centimeters [*Vogel et al.*, 2005]. The top of the accreted ice layer comprises a clear ice facies (Figure 4a) with either no debris or small amounts of dispersed particles (>2 m). The bottom is composed of solid dirty ice facies (Figure 4d), which is essentially a layer of frozen-on sediment (~0.6 m). A large middle section contains alternating layers composed of clear ice facies, laminated ice facies (Figure 4b) and massive dirty ice facies with sediment in suspension (Figure 4c). Physical characteristics of these four ice facies are outlined in Table 2. Image analysis with eCognition Professional and ArcGIS 9 suggest that debris contents for clear, laminated, massive and solid ice facies are 1%, 63%, 51%, and 66% by volume (Figures 4e–4h). These are likely upper estimates because ice transparency may lead us to overestimate the volumetric content of solid particles in 2-D imagery.

[20] Results of 15 model runs are summarized in a schematic facies diagram, Figure 5. Steady state development of clear facies (Figure 4a) occur if ice base and substrate are separated by basal water or if groundwater flows to the ice base fast enough to satisfy the basal freezing rate. Low to moderate freezing rates (~1–3 mm yr$^{-1}$) combined with a high but slightly insufficient rate of groundwater supply, say 90% of the freezing rate, should cause growth of a laminated facies (Figure 4b). More restricted water inflow should favor a massive facies (Figure 4c). Moderate to high freezing rates (3–6 mm yr$^{-1}$) and low water availability (<30%) should produce a solid dirty facies (Figure 4d).

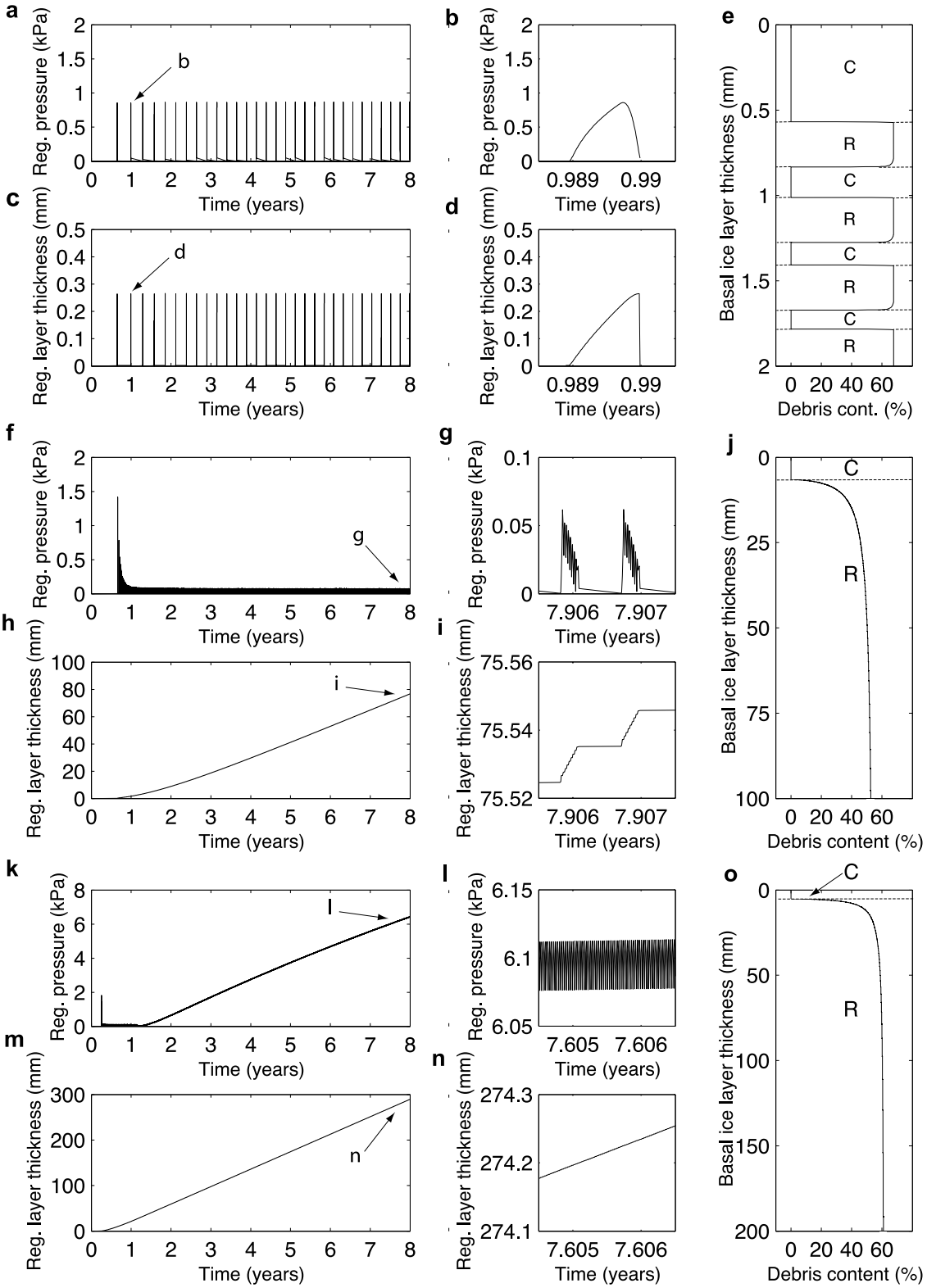


**Figure 3.** Model results showing regelation pressure and debris entrainment during accretion ice growth. (a–e) Model run 1 conducted with a basal ice temperature gradient of 0.04°C $m^{-1}$ and a water inflow of 95% of the freezing rate (1.4 mm $yr^{-1}$). (f–j) Model run 2 conducted with a basal ice temperature gradient of 0.05°C $m^{-1}$ and a water inflow of 50% of the freezing rate (3.6 mm $yr^{-1}$). (k–o) Model run 3 conducted with a basal ice temperature gradient of 0.06°C $m^{-1}$ (i.e., a freezing rate of 5.8 mm $yr^{-1}$) and no groundwater inflow. See text for details.

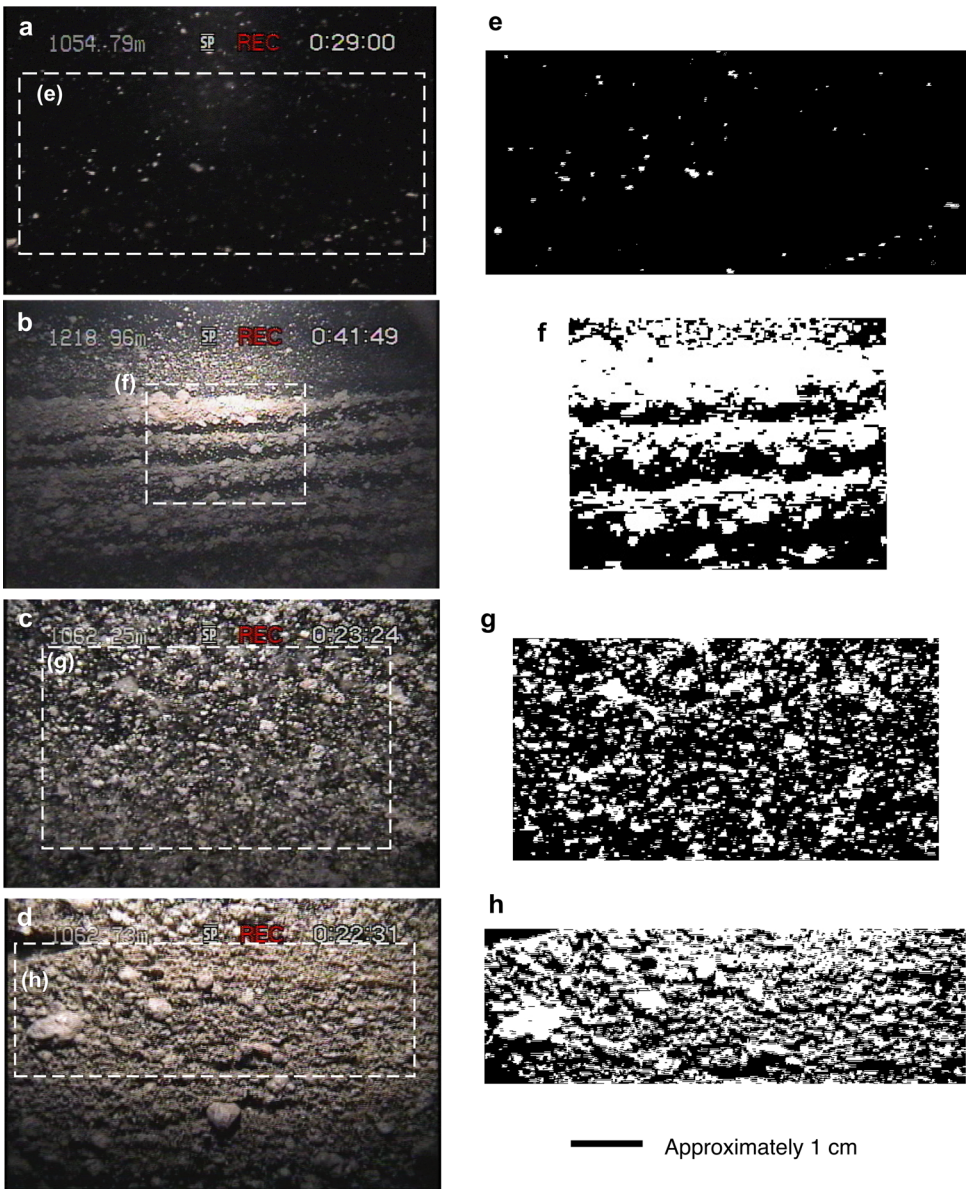


**Figure 4.** Images of basal ice facies observed in Kamb Ice Stream with the JPL borehole camera system. (left) Images of (a) clear ice facies, (b) laminated ice facies, (c) massive ice facies, and (d) solid ice facies. Each image covers approximately 4 cm in the vertical direction and up in image is down in borehole. (right) (e–h) Demonstration of how debris content was estimated from image analysis of picture segments whose borders are shown by dashed boxes in Figures 4a–4d. White denotes debris, and black illustrates clear ice.

[21] Our predicted thickness of debris laminas (~0.3–1.1 mm) is less than seen in Figure 4b and 6a (~1–5 mm) but the result is similar to observations of this facies elsewhere, e.g., *Hubbard and Sharp* [1995], who identified a laminated basal ice facies with debris thicknesses of 0.1–1 mm. Similar fine debris laminas are produced in frost heave experiments under unidirectional freezing [*Watanabe and Mizoguchi*, 2000; *Watanabe et al.*, 2001;

**Table 2.** Physical Character of Basal Ice Facies Observed in Kamb Ice Stream With JPL Borehole Camera System

| Facies | Description |
|---|---|
| Clear | clean, transparent ice; can contain dispersed debris or mud clots; debris content <1% |
| Laminated | clean, transparent ice with subhorizontal and regular debris laminas; debris content ~5–50% |
| Massive | debris and mud clots suspended uniformly in clean, transparent ice; debris content ~40–60% |
| Solid | clast-supported debris with clean interstitial ice; can contain ice lenses; debris content >60% |

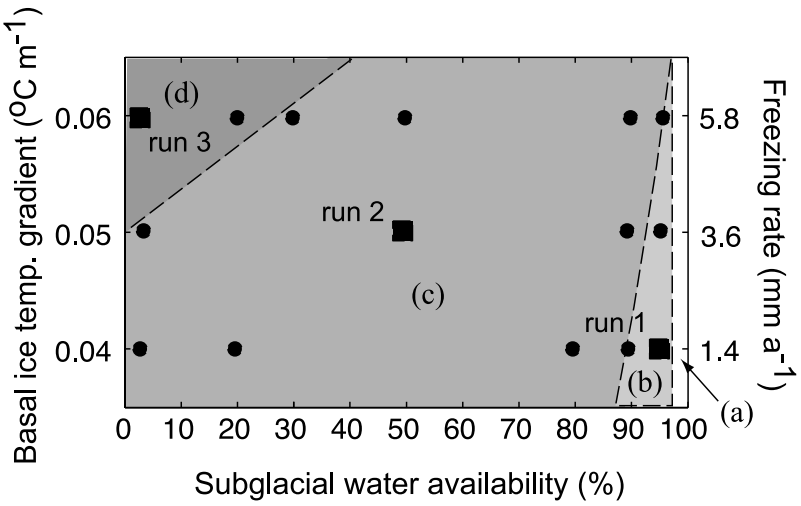


**Figure 5.** Schematic facies diagram illustrating subglacial conditions that should lead to basal ice facies as shown in Figures 4a–4d. Dots represent model simulations that are not discussed in text, while squares show model runs 1–3 discussed in the text.

*Watanabe*, 2002]. These laboratory experiments also show that increased solute concentration and increased freezing rate produce thinner ice lenses at lower temperatures [*Watanabe et al.*, 2001; *Watanabe*, 2002]. Sediment grain size distribution is also likely to control the configuration of ice lenses and debris bands [*Christoffersen and Tulaczyk*, 2003a]. It is thus not surprising that debris content of stratified basal ice facies can vary considerably. The estimate derived from Figure 4a (63%) is clearly higher than debris visible in Figure 6a (~5%), which may represent a lower end-member of the spectrum of debris concentrations for the stratified ice facies observed in Kamb Ice Stream. Values appear to range between 5 and 60%, which is comparable to debris concentrations for a banded ice facies (6–33%) observed at the coastal margin of Law Dome, East Antarctica [*Goodwin*, 1993]. Dispersed debris-poor and laminated facies also observed by *Goodwin* [1993] may correspond to the clear and debris-sparse, stratified facies observed highest in the accreted ice layer of Kamb Ice Stream (Figures 4a, 6a, and 6b). The predicted debris contents of massive dirty facies (~51%) and solid dirty facies (~63%) fit very well with values estimated from borehole camera images shown in Figure 4c (51%) and Figure 4d (66%). The latter facies is the equivalent of a frozen sedimentary layer. Comparable debris concentrations (30% and 47%) have been reported from suspended and solid facies observed in Greenland [*Waller et al.*, 2000]. Figure 6c shows that lenses of clean ice can develop within the solid facies through a segregation mechanism similar to frost heave. Ice lens development in subglacial sediments supports results from earlier work in which a frost-heave-based theory for basal freeze-on was first proposed [*Christoffersen and Tulaczyk*, 2003a] although that model did not contain the theoretical means to reproduce ice facies on a millimeter scale. The absence of dispersed facies in our model output is consistent with previous hypotheses suggesting that this facies is formed by a different mode related to either geological setting [*Sugden et al.*, 1987] or by deformation of ice with a stratified origin [*Knight*, 1994; *Waller et al.*, 2000]. The presence of dispersed debris in parts of the basal ice layer of Kamb Ice Stream (Figure 6b) may thus be evidence of postentrainment dispersal processes from localized ice deformation over protruding bedrock or frozen sticky spots [*Weertman*, 1968].

## 6. Discussion

[22] Our numerical investigations show that interactions between freeze-on and regelation may lead to formation of clear, stratified and solid basal ice facies when a freezing ice base overlies a layer of freshwater-saturated till. The four modeled ice facies highlighted above may well be associated with the stratified grouping within the two-facies interpretation proposed by *Lawson and Kulla* [1978] and adopted by *Knight* [1994] to encompass "solid" as well as "banded" ice facies observed in Greenland [e.g., *Sugden et al.*, 1987; *Souchez et al.*, 1993; *Tison et al.*, 1994]. However, we hesitate to fully adopt the two-facies classification because our model indicates that facies variability is more complex than put forward in that scheme. In our model the most important control on formation of different basal ice facies is the ratio of basal freezing rate to water supply rate. Clear basal ice facies with a very small debris content forms if water is freely available at the bed. Limitation in the water supply rate strengthens the ice-bed coupling and enhances the debris entrainment because the freezing interface moves downward, into the subglacial sediment, due to infiltration of ice by regelation. Clearly, we cannot rule out the possibility that processes not included in our model influence basal ice formation. However, within the physical framework of our model, we can use the basal ice layer from Kamb Ice Stream to infer a several thousand year record of subglacial conditions for one of the most dynamic parts of the West Antarctic Ice Sheet. The uppermost 1–4 m may have accreted under low freezing rates (~1 mm $yr^{-1}$) and very high meltwater availability (~100%). Higher freezing rates would require a highly pressurized groundwater system and/or ice-bed separation. A large middle section (6–10 m) accreted under fluctuating conditions characterized by low to moderate freez-

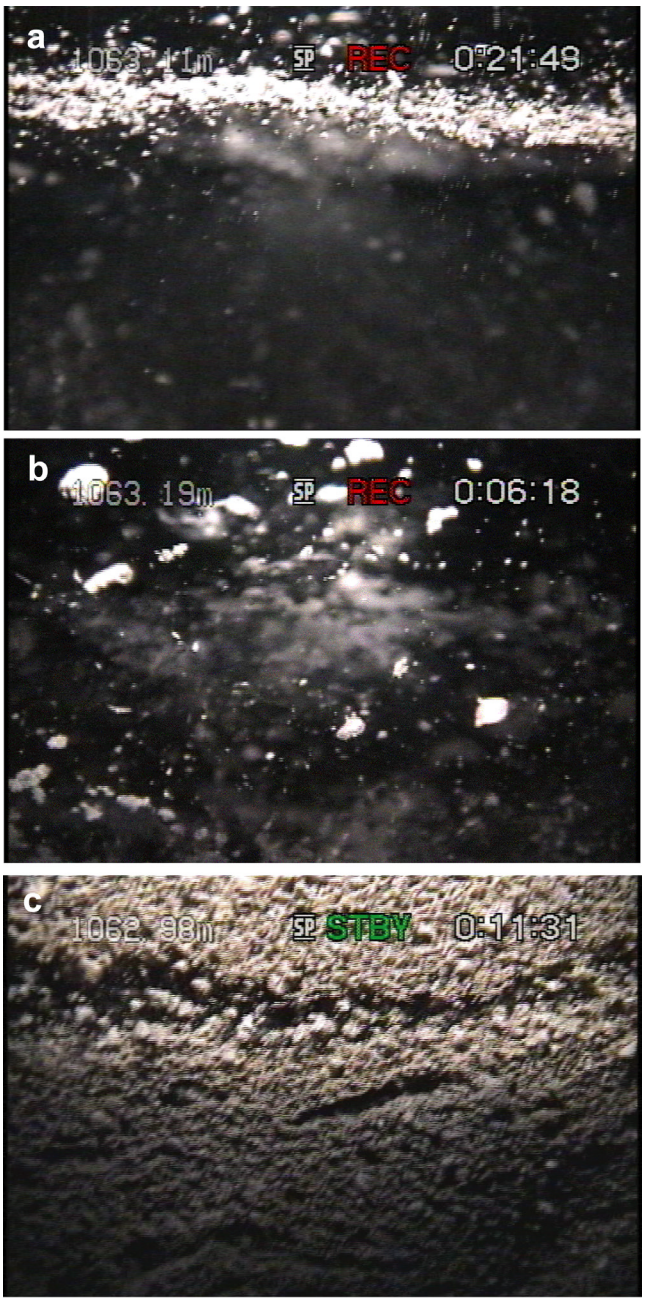


**Figure 6.** Borehole camera images of basal ice in Kamb Ice Stream. (a) Fine lamina of debris in clear ice. (b) Suspended particles in dispersed ice facies. (c) Ice lens formed in solid dirty facies. Each image covers about 4 cm in the vertical direction and up in image is down in borehole.

ing rates (1–3 mm $yr^{-1}$) and fluctuating but generally high water availability (>90%). Unconformities may exist in the accretion record due to periods of basal melting, and decimeter-thick units of dispersed ice facies may indicate either periods of sliding over crystalline bedrock or localized deformation [*Weertman*, 1961, 1968; *Hubbard and Sharp*, 1993, 1995]. The debris-rich bottom unit (~1–1.5 m) accreted under high freezing rates (>3 mm $yr^{-1}$) and critically restricted water conditions (<30%) i.e., conditions that most likely lead to ice stream stoppage ca. 150 years ago [*Vogel et al.*, 2005].

## 7. Conclusions

[23] Our model results provide a new quantitative framework for interpretation of basal ice facies formed by ice accretion over a subglacial till layer. Different basal ice facies should form in response to changes in freezing rate and subglacial water availability. We predict that clean and laminated basal ice facies form in the interior of ice sheets where meltwater is abundant. Massive dirty ice facies and solid dirty ice facies may form under cold basal conditions near ice margins or in ice streams if the basal ice temperature gradient becomes critically steep due to fast flow and ice thinning. The thick layer of debris-bearing basal ice in Kamb Ice Stream (>10 m) indicates that basal freezing is widespread and common, and a major agent for glacial erosion and sediment transfer, e.g., as proposed by *Iverson* [2000]. In our model sediment entrainment becomes significant when the basal freezing rate exceeds water supply rate. 300 years of water-depleted freezing at a rate of 5 mm $yr^{-1}$ could e.g., produce a 10-m-thick layer of debris-rich basal ice with a texture similar to frozen sediment (Figure 3m). We thus find that erosion rates beneath freezing stagnant ice in some cases (e.g., beneath stopped ice streams) may reach values similar to predictions for fast temperate ice motion [*Hallet et al.*, 1996]. This is consistent with estimates of debris entrainment following stoppage of Kamb Ice Stream [*Vogel et al.*, 2005]. Ice accretion in the interior of ice sheets may thus be an underestimated agent for glacial erosion and basal ice layers an underestimated source of glacial sedimentation. The geological significance of ice accretion processes are demonstrated by extensive ice-rafted debris in the North Atlantic [*Heinrich*, 1988; *Bond et al.*, 1992; *Bond and Lotti*, 1995].

## Appendix A

[24] We base our treatment of subglacial freezing on the frost-heave approach of *O'Neill and Miller* [1985] rather than the more recent frost-heave theory of *Rempel et al.* [2004]. Hence it is important to examine more closely the key quantitative difference between these two models. As pointed out by *Rempel et al.* [2004, p. 235], this key difference lies in the expression for the net interfacial force that causes frost heave:

$$F_T = \frac{F_T^{OM}}{z_l} \int_0^{z_l} (1 - \phi S_s) \partial z \qquad \text{(A1)}$$

where $F_T^{OM}$ is the net force as treated by *O'Neill and Miller* [1985], $z$ is vertical coordinate, $z_l$ is vertical coordinate of the active ice lens (as by *Rempel et al.* [2004, Figure 4]), $\phi$ is sediment porosity, $S_s$ is ice saturation. Note that *Rempel et al.* [2004] define $z = 0$ as the position where temperature is equal to the equilibrium temperature of phase transition in the absence of interfacial effects. Ice saturation is equal to one at $z = z_l$ and decreases to zero for $0 \leq z \leq z_f$, where $z_f$ is the vertical coordinate of the freezing front. Since we are not aware of any observational constraints on spatial

distribution of $S_s$, we express the distribution of ice saturation in a general power law, which satisfies the boundary conditions stated above and is valid over the domain $z_f \leq z \leq z_l$:

$$S_s = \left(\frac{z - z_f}{z_l - z_f}\right)^n \tag{A2}$$

where $n$ is an arbitrary exponent.

[25] To perform the integration in equation (A1) we express $z_f$ as a fraction of $z_l$, so that $z_f = kz_l$, where $k$ varies between 0 and 1. Under these conditions the difference between the treatment of interfacial force developed by *Rempel et al.* [2004] and that of *O'Neill and Miller* [1985] is

$$F_T = F_T^{OM}\left(1 - \frac{\phi(1-k)^n}{n+1}\right) \tag{A3}$$

[26] For typical porosities of subglacial till ranging between 0.2 and 0.4, the maximum difference for linear distribution of $S_s$ ($n = 1$ and $k = 0$) is just 10% and 20%, respectively. The difference decreases toward zero as $n \rightarrow \infty$ and $k \rightarrow 1$.

[27] *O'Neill and Miller*'s [1985] rigid ice model represents an end-member case of the model of *Rempel et al.* [2004] as the latter simplifies to the former when the influence of $S_s$ on interfacial force is null. Even when this is not the case, the difference between the two models is relatively minor. The rigid ice model offers a reasonable approximation of frost heave processes as observed in Nature and controlled laboratory experiments. The fundamental requirement for successful application of both models is that control parameters (e.g., distribution of ice saturation of *Rempel et al.* [2004] and interfacial curvature of *O'Neill and Miller* [1985]) are chosen to make model output match observations. The novel approach of *Rempel et al.* [2004] represents a microphysically correct generalization of the O'Neill and Miller's model but it does not overturn that theory. The limitations associated with using *O'Neill and Miller*'s [1985] treatment are in our model small compared to other uncertainties.

[28] **Acknowledgments.** Support for this study was provided by grants from the National Science Foundation Office of Polar Programs (NSF-OPP) and NASA to Slawek Tulaczyk. Frank D. Carsey and Alberto E. Behar performed their contribution at the Jet Propulsion Laboratory, California Institute of Technology, under contract with NASA. Poul Christoffersen acknowledges support from Carlsbergfondet. Acquisition of borehole imagery took place as part of a larger study funded by NSF-OPP grants to Barclay Kamb and Hermann Engelhardt, California Institute of Technology. We are grateful to both of them for their kind support. Editorial comments and reviews by Joseph Walder and an anonymous person were helpful.

## References

Alley, R. B., K. M. Cuffey, E. B. Evenson, J. C. Strasser, D. E. Lawson, and G. J. Larson (1997), How glaciers entrain and transport basal sediment: Physical constraints, *Quat. Sci. Rev.*, *16*, 1017–1038.

Alley, R. B., D. E. Lawson, E. B. Evenson, J. C. Strasser, and G. J. Larson (1998), Glaciohydraulic supercooling: A freeze-on mechanism to create stratified, debris-rich basal ice: II. Theory, *J. Glaciol.*, *44*, 563–569.

Anandakrishnan, S., and R. B. Alley (1997), Tidal forcing of basal seismicity of ice stream C, West Antarctica, observed far inland, *J. Geophys. Res.*, *102*(B7), 15,183–15,196.

Anandakrishnan, S., R. B. Alley, R. W. Jacobel, and H. Conway (2001), The flow regime of Ice Stream C and hypotheses concerning its recent stagnation, in *The West Antarctic Ice Sheet: Behavior and Environment*, *Antarct. Res. Ser.*, vol. 77, edited by R. B. Alley and R. A. Bindschadler, pp. 283–296, AGU, Washington, D. C.

Bindschadler, R. A., J. L. Bamber, and S. Anandakrishnan (2001), Onset of streaming flow in the Siple Coast region, West Antarctica, in *The West Antarctic Ice Sheet: Behavior and Environment*, *Antarct. Res. Ser.*, vol. 77, edited by R. B. Alley and R. A. Bindschadler, pp. 123–136, AGU, Washington, D. C.

Bindschadler, R. A., M. A. King, R. B. Alley, S. Anandakrishnan, and L. Padman (2003), Tidally controlled stick-slip discharge of a West Antarctic ice stream, *Science*, *301*, 1087–1089.

Bond, G., et al. (1992), Evidence for massive discharges of icebergs into the North-Atlantic Ocean during the last glacial period, *Nature*, *360*, 245–249.

Bond, G. C., and R. Lotti (1995), Iceberg discharges into the North-Atlantic on Millennial time scales during the last glaciation, *Science*, *267*, 1005–1010.

Bougamont, M., S. Tulaczyk, and I. Joughin (2003a), Numerical investigations of the slow-down of Whillans Ice Stream, West Antarctica: Is it shutting down like Ice Stream C?, *Ann. Glaciol.*, *37*, 239–246.

Bougamont, M., S. Tulaczyk, and I. Joughin (2003b), Response of subglacial sediments to basal freeze-on: 2. Application in numerical modeling of the recent stoppage of Ice Stream C, West Antarctica, *J. Geophys. Res.*, *108*(B4), 2223, doi:10.1029/2002JB001936.

Boulton, G. S., and U. Spring (1986), Isotopic fractionation at the base of polar and subpolar glaciers, *J. Glaciol.*, *32*, 475–485.

Carsey, F., A. Behar, A. L. Lane, V. Realmuto, and H. Engelhardt (2002), A borehole camera system for imaging the deep interior of ice sheets, *J. Glaciol.*, *48*, 622–628.

Christoffersen, P., and S. Tulaczyk (2003a), Response of subglacial sediments to basal freeze-on: 1. Theory and comparison to observations from beneath the West Antarctic Ice Sheet, *J. Geophys. Res.*, *108*(B4), 2222, doi:10.1029/2002JB001935.

Christoffersen, P., and S. Tulaczyk (2003b), Thermodynamics of basal freeze-on: Predicting basal and subglacial signatures of stopped ice streams and interstream ridges, *Ann. Glaciol.*, *36*, 233–243.

Clarke, G. K. C. (1987), Subglacial till: A physical framework for its properties and processes, *J. Geophys. Res.*, *92*, 9,023–9,036.

Clarke, G. K. C. (2005), Subglacial processes, *Annu. Rev. Earth Planet. Sci.*, *33*, 247–276.

Clarke, G. K. C., and E. W. Blake (1991), Geometric and thermal evolution of a surge-type glacier in its quiescent state: Trapridge Glacier, Yukon Territory, Canada, *J. Glaciol.*, *37*, 158–169.

Copland, L., M. J. Sharp, and P. W. Nienow (2003), Links between short-term velocity variations and the subglacial hydrology of a predominantly cold polythermal glacier, *J. Glaciol.*, *49*, 337–348.

Cuffey, K. M., H. Conway, A. M. Gades, B. Hallet, R. Lorrain, J. P. Severinghaus, E. J. Steig, B. Vaughn, and J. W. C. White (2000), Entrainment at cold glacier beds, *Geology*, *28*, 351–354.

Domenico, P. A., and F. W. Schwartz (1990), *Physical and Chemical Hydrogeology*, 824 pp., John Wiley, Hoboken, N. J.

Engelhardt, H. (2004), Ice temperature and high geothermal flux at Siple Dome, West Antarctica, from borehole measurements, *J. Glaciol.*, *50*, 251–256.

Engelhardt, H., and B. Kamb (1997), Basal hydraulic system of a West Antarctic ice stream: Constraints from borehole observations, *J. Glaciol.*, *43*, 207–230.

Engelhardt, H., and B. Kamb (1998), Basal sliding of Ice Stream B, West Antarctica, *J. Glaciol.*, *44*, 223–230.

Flowers, G. E., and G. K. C. Clarke (2002), A multicomponent coupled model of glacier hydrology: 2. Application to Trapridge Glacier, Yukon, Canada, *J. Geophys. Res.*, *107*(B11), 2288, doi:10.1029/2001JB001124.

Fowler, A. C., and W. B. Krantz (1994), A generalized secondary frost heave model, *SIAM J. Appl. Math.*, *54*, 1650–1675.

Goodwin, I. D. (1993), Basal ice accretion and debris entrainment within the coastal ice margin, Law Dome, Antarctica, *J. Glaciol.*, *39*, 157–166.

Gow, A. J., S. Epstein, and W. Sheeny (1979), On the origin of stratified debris in ice cores from the bottom of the Antarctic ice sheet, *J. Glaciol.*, *23*, 185–192.

Gregg, S. J., and K. S. W. Sing (1982), *Adsorption, Surface Area and Porosity*, 2nd ed., 303 pp., Elsevier, New York.

Hallet, B., L. Hunter, and J. Bogen (1996), Rates of erosion and sediment evacuation by glaciers: A review of field data and their implications, *Global Planet. Change*, *12*, 213–235.

Heinrich, H. (1988), Origin and consequences of cyclic ice rafting in the Northeast Atlantic Ocean during the past 130,000 years, *Quat. Res.*, *29*, 142–152.

Herron, S., and C. C. J. Langway (1979), The debris-laden ice at the bottom of the Greenland Ice Sheet, *J. Glaciol.*, *23*, 193–208.
Hooke, R. L. (1998), *Principles of Glacier Mechanics*, 248 pp., Prentice-Hall, Upper Saddle River, N. J.
Hubbard, B., and M. Sharp (1993), Weertman regelation, multiple refreezing events and the isotopic evolution of the basal ice layer, *J. Glaciol.*, *39*, 275–291.
Hubbard, B., and M. Sharp (1995), Basal ice facies and their formation in the western Alps, *Arct. Alp. Res.*, *27*, 301–310.
Iverson, N. R. (1993), Regelation of ice through debris at glacier beds: Implications for sediment transport, *Geology*, *21*, 559–562.
Iverson, N. R. (2000), Sediment entrainment by a soft-bedded glacier: A model based on regelation into the bed, *Earth Surf. Processes Landforms*, *25*, 881–893.
Iverson, N. R., and D. J. Semmens (1995), Intrusion of ice into porous media by regelation: A mechanism of sediment entrainment by glaciers, *J. Geophys. Res.*, *100*(B6), 10,219–10,230.
Jouzel, J., et al. (1999), More than 200 meters of lake ice above subglacial lake Vostok, Antarctica, *Science*, *286*, 2138–2141.
Kamb, B. (1991), Rheological nonlinearity and flow instability in the deforming bed mechanism of ice stream motion, *J. Geophys. Res.*, *96*(B9), 16,585–16,595.
Kamb, B. (2001), Basal zone of the West Antarctic ice streams and its role in lubrication of their rapid motion, in *The West Antarctic Ice Sheet: Behavior and Environment*, *Antarct. Res. Ser.*, vol. 77, edited by R. B. Alley and R. A. Bindschadler, pp. 157–201, AGU, Washington, D. C.
Knight, P. G. (1994), 2-facies interpretation of the basal layer of the Greenland Ice Sheet contributes to a unified model of basal ice formation, *Geology*, *22*, 971–974.
Knight, P. G. (1997), The basal ice layer of glaciers and ice sheets, *Quat. Sci. Rev.*, *16*, 975–993.
Krantz, W. B., and K. E. Adams (1996), Application of a fully predictive model for secondary frost heave, *Arct. Alp. Res.*, *28*, 284–293.
Lawson, D. E., and J. B. Kulla (1978), An oxygen isotope investigation of the origin of the basal zone of the Matanuska Glacier, Alaska, *J. Geol.*, *86*, 673–685.
Lawson, D. E., J. C. Strasser, E. B. Evenson, R. B. Alley, G. J. Larson, and S. A. Arcone (1998), Glaciohydraulic supercooling: A freeze-on mechanism to create stratified, debris-rich basal ice: I. Field evidence, *J. Glaciol.*, *44*, 547–562.
Miller, R. D. (1973), Soil freezing in relation to pore water pressure and temperature, paper presented at 2nd International Conference on Permafrost, Natl. Acad. Sci., Yakutsk, Russia.
Miyata, Y. (1998), A thermodynamic study of liquid transportation in freezing porous media, *JSME Int. J. Ser. B*, *41*, 601–609.
Miyata, Y., and S. Akagawa (1998), An experimental study of dynamic solid-liquid phase equilibrium in a porous medium, *JSME Int. J. Ser. B*, *41*, 590–600.
O'Neill, K. (1983), The physics of mathematical frost heave models: A review, *Cold Reg. Sci. Technol.*, *6*, 275–291.
O'Neill, K., and R. D. Miller (1985), Exploration of a rigid ice model of frost heave, *Water Resour. Res.*, *21*, 281–296.
Raymond, C. F., and W. D. Harrison (1975), Some observations on the behavior of the liquid and gas phases in temperate glacier ice, *J. Glaciol.*, *14*, 213–234.
Raymond, C. F., K. A. Echelmeyer, I. M. Whillans, and C. S. M. Doake (2001), Ice stream shear margins, in *The West Antarctic Ice Sheet: Behavior and Environment*, *Antarct. Res. Ser.*, vol. 77, edited by R. B. Alley and R. A. Bindschadler, pp. 137–156, AGU, Washington, D. C.
Rempel, A. W., J. S. Wettlaufer, and M. G. Worster (2004), Premelting dynamics in a continuum model of frost heave, *J. Fluid Mech.*, *498*, 227–244.
Roberts, M. J., F. S. Tweed, A. J. Russell, O. Knudsen, D. E. Lawson, G. J. Larson, E. B. Evenson, and H. Bjornsson (2002), Glaciohydraulic supercooling in Iceland, *Geology*, *30*, 439–442.
Souchez, R., J. L. Tison, and J. Jouzel (1987), Freezing rate determination by the isotopic composition of the ice, *Geophys. Res. Lett.*, *14*, 599–602.
Souchez, R., M. Lemmens, J. L. Tison, R. Lorrain, and L. Janssens (1993), Reconstruction of basal boundary-conditions at the Greenland Ice-Sheet margin from gas-composition in the ice, *Earth Planet. Sci. Lett.*, *118*, 327–333.
Souchez, R., P. Jean-Baptiste, J. R. Petit, V. Y. Lipenkov, and J. Jouzel (2003), What is the deepest part of the Vostok ice core telling us?, *Earth Sci. Rev.*, *60*, 131–146.
Souchez, R., D. Samyn, R. Lorrain, F. Pattyn, and S. Fitzsimons (2004), An isotopic model for basal freeze-on associated with subglacial upward flow of pore water, *Geophys. Res. Lett.*, *31*, L02401, doi:10.1029/2003GL018861.
Sugden, D. E., P. G. Knight, N. Livesey, R. D. Lorrain, R. A. Souchez, J. L. Tison, and J. Jouzel (1987), Evidence for 2 zones of debris entrainment beneath the Greenland Ice Sheet, *Nature*, *328*, 238–241.
Tison, J. L., T. Thorsteinsson, R. D. Lorrain, and J. Kipfstuhl (1994), Origin and development of textures and fabrics in basal ice at Summit, central Greenland, *Earth Planet. Sci. Lett.*, *125*, 421–437.
Tulaczyk, S. (1999), Ice sliding over weak, fine-grained tills: Dependence of ice-till interaction on till granulometry, in *Glacial Processes, Past and Modern*, edited by D. M. Mickelson and J. Attig, *Spec. Pap. Geol. Soc. Am.*, 337, 159–177.
Tulaczyk, S., B. Kamb, R. P. Scherer, and H. F. Engelhardt (1998), Sedimentary processes at the base of a West Antarctic ice stream: Constraints from textural and compositional properties of subglacial debris, *J. Sediment. Res.*, *68*, 487–496.
Tulaczyk, S., W. B. Kamb, and H. F. Engelhardt (2000), Basal mechanics of Ice Stream B, West Antarctica: 1. Till mechanics, *J. Geophys. Res.*, *105*(B1), 463–481.
Tulaczyk, S., B. Kamb, and H. F. Engelhardt (2001), Estimates of effective stress beneath a modern West Antarctic ice stream from till preconsolidation and void ratio, *Boreas*, *30*, 101–114.
Vogel, S. W., S. Tulaczyk, B. Kamb, H. Engelhardt, F. D. Carsey, A. E. Behar, A. L. Lane, and I. Joughin (2005), Subglacial conditions during and after stoppage of an Antarctic Ice Stream: Is reactivation imminent?, *Geophys. Res. Lett.*, *32*, L14502, doi:10.1029/2005GL022563.
Waller, R. I., J. K. Hart, and P. G. Knight (2000), The influence of tectonic deformation on facies variability in stratified debris-rich basal ice, *Quat. Sci. Rev.*, *19*, 775–786.
Watanabe, K. (2002), Relationship between growth rate and supercooling in the formation of ice lenses in a glass powder, *J. Cryst. Growth*, *237*, 2194–2198.
Watanabe, K., and M. Mizoguchi (2000), Ice configuration near a growing ice lens in a freezing porous medium consisting of micro glass particles, *J. Cryst. Growth*, *213*, 135–140.
Watanabe, K., Y. Muto, and M. Mizoguchi (2001), Water and solute distributions near an ice lens in a glass-powder medium saturated with sodium chloride solution under unidirectional freezing, *Cryst. Growth Des.*, *1*, 207–211.
Weertman, J. (1961), Mechanism for the formation of inner moraines found near the edge of cold ice caps and ice sheets, *J. Glaciol.*, *3*, 965–978.
Weertman, J. (1964), Glacier sliding, *J. Glaciol*, *5*, 287–303.
Weertman, J. (1968), Diffusion law for the dispersion of hard particles in an ice matrix that undergoes simple shear deformation, *J. Glaciol.*, *7*, 161–165.

A. E. Behar and F. D. Carsey, Jet Propulsion Laboratory, California Institute of Technology, 4800 Oak Grove Drive, Pasadena, CA 91109, USA.

P. Christoffersen, Centre for Glaciology, Institute of Geography and Earth Sciences, University of Wales, Aberystwyth SY23 3DB, UK. (pac@aber.ac.uk)

S. Tulaczyk, Department of Earth Sciences, University of California, Santa Cruz, CA 95064, USA.